Iron and citrate export by a major facilitator superfamily pump regulates metabolism and stress resistance in *Salmonella* Typhimurium

Elaine R. Frawley[a], Marie-Laure V. Crouch[a,1], Lacey K. Bingham-Ramos[a], Hannah F. Robbins[a], Wenliang Wang[b], Gerard D. Wright[b], and Ferric C. Fang[a,c,2]

Departments of [a]Laboratory Medicine and [c]Microbiology, University of Washington, Seattle, WA 98195; and [b]Michael G. DeGroote Institute for Infectious Disease Research, McMaster University, Hamilton, ON, Canada L8S 4L8

Edited by Hiroshi Nikaido, University of California, Berkeley, CA, and approved June 13, 2013 (received for review October 22, 2012)

The efficacy of antibiotics and host defenses has been linked to the metabolic and redox states of bacteria. In this study we report that a stress-induced export pump belonging to the major facilitator superfamily effluxes citrate and iron from the enteric pathogen *Salmonella* Typhimurium to arrest growth and ameliorate the effects of antibiotics, hydrogen peroxide, and nitric oxide. The transporter, formerly known as MdtD, is now designated IceT (iron citrate efflux transporter). Iron efflux via an iron-chelating tricarboxylic acid cycle intermediate provides a direct link between aerobic metabolism and bacterial stress responses, representing a unique mechanism of resistance to host defenses and antimicrobial agents of diverse classes.

antibiotic resistance | oxidative stress

Increasing rates of resistance and a dwindling pipeline of novel agents have focused renewed attention on mechanisms of intrinsic resistance to antibiotics. Studies have suggested that bacterial killing by antibiotics belonging to diverse functional classes is mediated in part by interaction with aerobic metabolic pathways, generation of reactive oxygen species (ROS), and iron-catalyzed Fenton chemistry (1–5). Though recent work demonstrated bactericidal activity of antibiotics in the absence of ROS and failed to detect peroxide or superoxide generation in response to treatment, it remains likely that iron availability and the metabolic state of the cell influence antibiotic susceptibility (6, 7).

Iron is an essential metal in nearly all living organisms, serving as a cofactor for proteins involved in redox chemistry and electron transport (8, 9); it is generally considered a limited resource for pathogenic bacteria such as *Salmonella enterica* serovar Typhimurium (*S.* Typhimurium), and iron availability is an important determinant of virulence. Iron-deficient mice are more resistant to *S.* Typhimurium infection, and increased systemic iron concentrations correlate with increased bacterial growth, adhesion, invasion, and lethality (10–12). Though the host requires some iron to generate an antimicrobial oxidative burst, iron restriction is an important defense strategy (13). Host organisms use numerous mechanisms to sequester iron from invading microbes, and many studies have focused on the high-affinity uptake systems that bacteria use to obtain iron in the metal-restricted host environment (14–18). Little attention has been paid to the question of whether bacteria might excrete iron under stress conditions to limit iron-dependent cytotoxicity. The same redox properties that allow iron to fulfill diverse biochemical roles present a danger if iron is not incorporated into enzymes or bound by storage proteins. Free cytoplasmic iron can participate in oxidative Fenton chemistry to generate radicals capable of damaging proteins and DNA (19–23) and potentiate the antimicrobial actions of ROS and reactive nitrogen species (RNS) (24–27).

In this study, a screen for mutations that enhanced susceptibility of *S.* Typhimurium to the iron-dependent antibiotic streptonigrin (SN) yielded transposon insertions in an operon encoding a two-component regulatory system (BaeSR), a drug efflux system belonging to the resistance-nodulation-division superfamily (MdtABC), and a putative transporter in the major facilitator superfamily (MdtD). Biochemical analysis demonstrated that MdtD promotes the efflux of citrate, an iron-chelating tricarboxylic acid cycle intermediate; hence, MdtD is renamed IceT, for Iron-citrate efflux Transporter. IceT expression lowers cellular iron content, arrests bacterial growth, and confers resistance to hydrogen peroxide, nitric oxide, and antibiotics from diverse functional classes.

Results

Transposon Insertions in the *mdtABCD baeSR* Operon Enhance Susceptibility to Streptonigrin. To search for candidate genes affecting intracellular free iron concentrations, a MudJ transposon mutant library was screened for hypersensitivity to SN, which requires intracellular reduction and oxygen for its bactericidal activity (28). The activity of SN depends on intracellular iron availability; siderophore and iron-uptake mutants are highly resistant to SN, whereas iron supplementation and restored iron uptake lead to enhanced SN activity. Additionally, iron chelators protect cells against SN. Three SN-hypersensitive mutants were found to contain independent transposon insertions in *mdtB*, the second gene in the *mdtABCD baeSR* operon (Fig. 1). This operon encodes a resistance–nodulation–division (RND) drug efflux pump (MdtABC), an uncharacterized transporter in the major facilitator superfamily (MFS) group (MdtD), and a two-component regulatory system (BaeSR) that has been shown to regulate expression of its own operon as well as the multidrug transporter *acrD*, periplasmic chaperone *spy*, and genes of unknown function, *yicO* and *ygcL*. (29–31). A role for *mdtABC* in resistance to novobiocin, bile salts, deoxycholate, and β-lactam antibiotics has been demonstrated, and a role in transport of flavenoids and sodium tungstate has been suggested (29–33). MdtD is a predicted cytoplasmic membrane protein with 12–14 transmembrane domains. By sequence homology, MdtD belongs to the drug:proton antiporter-2 (DHA2) subfamily, although it has not been shown to contribute to drug resistance phenotypes associated with the operon. Because a function for MdtABC had already been determined, whereas the function of MdtD has remained unknown, and because other classes of MFS

Author contributions: E.R.F., M.-L.V.C., L.K.B.-R., H.F.R., W.W., G.D.W., and F.C.F. designed research; E.R.F., M.-L.V.C., L.K.B.-R., H.F.R., and W.W. performed research; E.R.F., M.-L.V.C., L.K.B.-R., W.W., G.D.W., and F.C.F. analyzed data; and E.R.F. and F.C.F. wrote the paper.

The authors declare no conflict of interest.

This article is a PNAS Direct Submission.

[1]Present address: Albany Molecular Research, Inc., Bothell, WA 98021.

[2]To whom correspondence should be addressed. E-mail: fcfang@uw.edu.

This article contains supporting information online at www.pnas.org/lookup/suppl/doi:10.1073/pnas.1218274110/-/DCSupplemental.

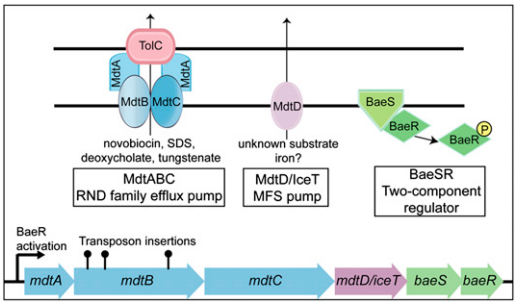

Fig. 1. MudJ transposon insertions in *mdtABCD baeSR* confer streptonigrin sensitivity. A screen for *S.* Typhimurium mutants with enhanced SN sensitivity identified three independent insertions in *mdtB*. The *mdtABCD baeSR* operon encodes an RND-family efflux pump (MdtABC) that forms a complex with TolC to efflux substrates, an uncharacterized MFS pump (MdtD/IceT), and a two-component regulatory system (BaeSR).

transporters have been implicated in the influx or efflux of a wide range of small molecules, including iron siderophores and nickel, MdtD was investigated as a candidate iron efflux transporter.

Expression of MdtD(IceT) Is Directly Related to Streptonigrin Resistance. To determine whether part of the SN-susceptibility phenotype observed in the transposon mutant screen was attributable to the loss of MdtD expression, a Δ*mdtD*(*iceT*) *S.* Typhimurium mutant (EF221) was constructed. Both EF221 and an isogenic WT strain (EF3) grew identically in LB, but in 6 μg mL^{-1} SN, the Δ*mdtD*(*iceT*) mutant was delayed in exiting lag phase (Fig. 2*A*, dashed green line), indicating enhanced sensitivity to the antibiotic. To examine the extent of this growth defect, EF3 and EF221 were grown in a range of SN concentrations. The defect was small but present at 4 μg mL^{-1} SN, and increased at higher SN concentrations (Fig. S1). Though slightly larger growth defects could be observed at 8 μg mL^{-1} and 10 μg mL^{-1}, the growth defect was most consistent at 6 μg mL^{-1} SN. The defect was complemented by expressing *mdtD*(*iceT*) from the native *mdtA* promoter (Fig. 2*B*). To further explore the SN phenotype of an *mdtD*(*iceT*) mutant, an SN killing assay was performed in which EF3 and EF221 were grown to OD_{600} 0.5–0.6 (50% maximum OD as determined in Fig. 2*A*), treated with 10 μg mL^{-1} SN and assayed for survival by plating and enumeration of colony forming units (cfu). No significant survival difference was observed between WT and the mutant, which might be attributable to the very low levels of *mdtD*(*iceT*) expression observed under basal conditions. Therefore, the killing assay was repeated in a Δ*fur* mutant background in which iron homeostasis is disrupted (EF394 and EF395), and a modest (1.7-fold) but significant decrease in survival was observed in the Δ*fur* Δ*mdtD*(*iceT*) strain (Fig. 2*C*). When cells containing empty vector (EF39) or an MdtD(IceT) expression vector (EF35) were induced with 1 mM IPTG before treatment with 10 μg mL^{-1} SN, the MdtD(IceT)-expressing cells displayed increased survival compared with WT cells (Fig. 2*D*, dark blue and green bars). To confirm that the killing by SN was iron dependent, the assay was repeated in the presence of the iron chelator *o*-phenanthroline. Addition of 0.1 mM *o*-phenanthroline protected cells from killing (Fig. 2*D*, light blue and green bars).

The *mdtABCD baeSR* Operon Is Induced by Nitric Oxide and Disruption of Iron Homeostasis. A variety of inducing conditions have been suggested for the *mdtABCD baeSR* operon (30, 33–35). We determined whether host cell-derived antimicrobial mediators such as nitric oxide (NO·), superoxide, or hydrogen peroxide, which can target iron centers and promote Fenton chemistry, are capable of inducing *mdtABCD baeSR* expression. Although an *mdtD*(*iceT*) mutant was more susceptible to hydrogen peroxide under conditions of enhanced iron uptake, and MdtD(IceT) expression protected cells against hydrogen peroxide treatment (Fig. S2), neither hydrogen peroxide nor paraquat, a redox-cycling agent and superoxide generator, significantly induced expression of the *mdtABCD baeSR* operon. However, NO· released from diethylamine NONOate (DEA/NO) was found to induce *mdtABCD baeSR* expression in a BaeSR-dependent manner (Fig. 3*A*). Growth curves of EF3 and EF221 were superimposable in the absence of an NO· donor, but when cells were treated with a combination of 1 mM DEA/NO and 2 mM spermine NONOate (Sper/NO) to generate a sustained NO· flux, the Δ*mdtD*(*iceT*) mutant was delayed in exiting lag phase, indicating enhanced sensitivity to NO· (Fig. 3*B*). To determine whether the *mdtABCD baeSR* operon is induced under conditions of iron stress, expression was examined in an isogenic Δ*fur* mutant (EF394) in which iron uptake systems were constitutively expressed. A previous study to identify iron-responsive genes in *S.* Typhimurium failed to detect a response of the *mdtABCD baeSR* operon to iron restriction or supplementation per se (36). Therefore, disrupted iron homeostasis in a Δ*fur* mutant, rather

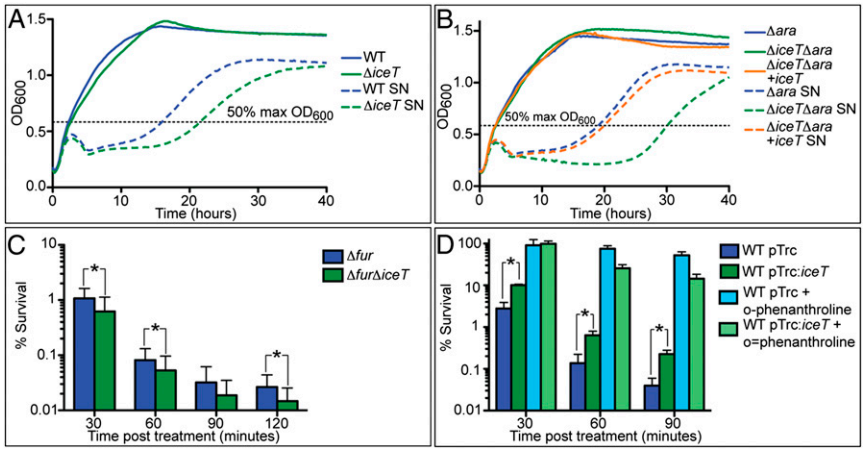

Fig. 2. Expression of MdtD(IceT) is directly related to streptonigrin resistance. (*A*) In the absence of SN, EF221 [Δ*mdtD*(*iceT*); solid green line] grows as well as isogenic WT strain EF3 (solid blue line). In 6 μg mL^{-1} SN, the mutant strain exhibits delayed exit from lag phase (dashed green line). Mean lag-time for EF221 to reach 50% max OD_{600} (horizontal dashed line) was 5.73 h, $P = 0.026$. (*B*) An insertion in the *araBAD* locus does not affect growth of EF390 (blue), EF391 (green), and EF393 (orange) in LB (solid lines). In 6 μg mL^{-1} SN, expression of *mdtD*(*iceT*) under control of its native P_{mdtA} promoter in strain EF393 (dashed orange line) complements the growth defect of EF391 [Δ*mdtD*(*iceT*), dashed green line], with similar growth to EF390, which contains an intact *mdtD* (*iceT*) gene (dashed blue line). (*C*) EF395 [Δ*fur* Δ*mdtD*(*iceT*)] is more susceptible to killing by 10 μg mL^{-1} SN than EF394 (Δ*fur*) at 30 min $P = 0.032$, 60 min $P = 0.008$, 90 min $P = 0.08$, and 120 min $P = 0.006$. (*D*) EF35 (dark green columns) expressing *mdtD*(*iceT*) is more resistant to killing by 10 μg mL^{-1} SN than EF39 (dark blue columns) containing empty vector at 30 min $P = 0.0008$, 60 min $P = 0.0088$, and 90 min $P = 0.0046$. Addition of 0.1 mM *o*-phenanthroline, an iron chelator, abrogated SN-killing in both strains (light blue and light green columns). Growth curves (*A* and *B*) are an average of seven experiments. Killing data are the mean of eight (*C*) and four (*D*) replicates ±1 SD. Statistical significance (*) was determined by two-tailed *t* test.

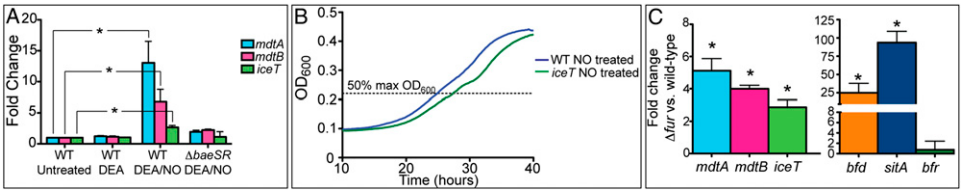

Fig. 3. The *mdtABCD baeSR* operon is induced by NO· stress and disrupted iron homeostasis. (*A*) EF3 (WT) and EF214 (Δ*baeSR*) were treated with 1 mM DEA mock treatment or 1 mM NO· DEA/NO and expression of *mdtA*, *mdtB*, and *mdtD*(*iceT*) assayed by qPCR. In the WT background, genes were significantly up-regulated upon DEA/NO treatment ($P < 0.006$). In the Δ*baeSR* background, only a modest residual level of induction was observed ($P < 0.05$). (*B*) EF3 and EF221 were grown in 1 mM DEA/NO and 2 mM Sper/NO. The Δ*mdtD*(Δ*iceT)* mutant (green line) exhibited delayed exit from lag phase. Mean lag time for EF221 to reach 50% max OD_{600} (dashed line) was 2.9 h ($P = 0.013$). (*C*) Expression of *mdtA*, *mdtB*, and *mdtD*(*iceT*) was compared in EF394 (Δ*fur*) and EF3 (WT) by qPCR and shown to be significantly up-regulated ($P < 0.03$). Expression of *bfd*, *sitA*, and *bfr* was measured as a control for Fur-dependent gene expression. Expression data are the mean of three replicates ±1 SD with significance (*) determined by two-tailed *t* test. Growth curves are an average of five experiments with significance determined by paired two-tailed *t* test.

than direct regulation by Fur, may lead to *mdtABCD baeSR* expression (Fig. 3*C*). To confirm the anticipated patterns of gene expression in the Δ*fur* mutant, expression of *bfd*, *sitA*, and *bfr* were also determined. As expected, expression of the Fur-repressed *bfd* and *sitA* genes was elevated in the Δ*fur* mutant, whereas expression of *bfr* was essentially unchanged, which may reflect the low levels of *bfr* expression observed during the exponential phase of growth (36–38).

Cells Expressing MdtD(IceT) Are More Resistant to Iron-Mediated Killing and Have Reduced Total Cellular Iron Content. Iron uptake and storage are highly regulated to limit the cytotoxicity of free intracellular iron. To examine the role of MdtD(IceT) under stress conditions in which intracellular free iron is elevated, strains expressing the FeoAB iron uptake system were grown in 2 mM $FeSO_4$. HR112, coexpressing MdtD(IceT), exhibited an ~2 $\log_{10}$ survival difference over HR111 containing empty vector (Fig. 4*A*).

To determine whether enhanced survival resulted from reduced iron levels, total iron content of HR111 and HR112 was measured by inductively coupled plasma-mass spectrometry (ICP-MS). Cells were grown 1 mM $FeSO_4$ to reduce the amount of cell death from iron-catalyzed oxidative damage. Following 30-min iron exposure, HR112 had a 50% reduction in total iron content compared with HR111 (Fig. 4*B*). Other transition metals were not affected by MdtD(IceT) expression (Fig. S3*A*). Lower levels of total iron were also found in EF35, expressing only MdtD(IceT), compared with EF39, although the difference was more modest, most likely due to lower amounts of free iron available for export in the absence of FeoAB overexpression (Fig. S3*B*).

To examine the effect of MdtD(IceT) expression over time, FeoAB expression was induced in HR111 and HR112, and 1 mM $FeSO_4$ was added 30 min before the induction of MdtD(IceT) expression. Total cellular iron content was analyzed at 30-min intervals beginning at the time of iron addition. Both HR111 and HR112 accumulated similar amounts of iron upon $FeSO_4$ addition and experienced slight but identical drops in total iron content immediately post-IPTG induction. However, at 60 and 90 min postinduction of MdtD(IceT), the total iron content of HR111 rose, and the iron content of HR112 continued to decline. The difference in iron content between the strains is significant at these time points and is likely an underestimate of the true difference in total iron because enumeration of cfu indicated greater survival of IceT-overexpressing HR112 cells following iron exposure.

MdtD(IceT) Exports the Iron Chelator Citrate. Iron is typically translocated in complex with a protein or chelating molecule. After obtaining data showing that MdtD(IceT) expression leads to lower intracellular iron content, we sought to determine whether MdtD(IceT) mediates export of an iron chelator using the chrome azurol S (CAS) reagent (39). CAS binds iron with relatively low affinity and is normally blue in color. Upon donation of iron to a chelator of higher affinity, CAS undergoes a color change to orange. Experiments were performed using Δ*entB* strains incapable of producing iron-chelating siderophores (18). EF341 and EF342 were grown in M9 medium supplemented with casamino acids, and then cell-free spent medium was combined 1:1 with CAS reagent. For samples containing a chelator, an obvious color change is detectable after 5–10 min. Medium from cultured Δ*entB* cells containing empty vector (EF341) was CAS-negative, as anticipated (Fig. 5*A*, lane 1). However, medium from cultured Δ*entB* cells expressing MdtD (IceT, EF342) was CAS-positive (Fig. 5*A*, lane 2), indicating that MdtD(IceT) expression leads to the secretion of an iron chelator unrelated to the two known *S.* Typhimurium catecholate siderophores enterobactin and salmochelin. Secretion of this chelator was specific to MdtD(IceT), because culture medium from EF336 expressing MdtABC was CAS-negative. To confirm that the presence of a CAS-positive chelator in the medium was not due to a loss of membrane integrity, EF341, EF342, and EF336 were stained with SYTO9 and propidium iodide and verified to have intact cell membranes (Fig. S4). To identify the chelator, spent medium from EF341 and EF342 cultures was subjected to chromatography over a series of columns with various eluants to purify the CAS-reactive component. No CAS-reactive molecule was identified in supernatant from the EF341 control culture.

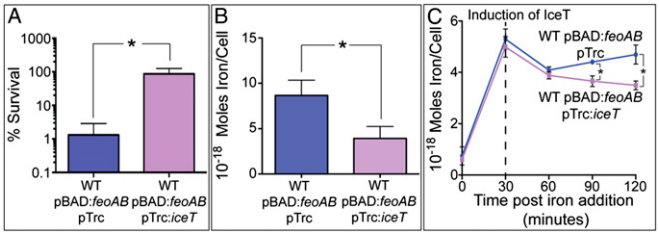

Fig. 4. Cells expressing MdtD(IceT) are resistant to iron-mediated cell death and have reduced total iron content. (*A*) Strains HR111 and HR112 expressing the FeoAB iron import system were grown in LB containing 2 mM $FeSO_4$ for 30 min. HR112 expressing MdtD(IceT) (purple) better survived iron challenge by almost 2 $\log_{10}$ compared with HR111 containing empty vector (blue). (*B*) HR111 and HR112 were grown in 1 mM $FeSO_4$ for 30 min before total iron content was determined by ICP-MS. HR111 (blue) contained more than twice as much iron as HR112 (purple). (*C*) HR111 and HR112 were induced for FeoAB expression, then grown in 1 mM $FeSO_4$ for 30 min before MdtD(IceT) expression was induced. Iron content was determined by ICP-MS at 30-min intervals post-iron addition. All data are the mean of three replicates ±1 SD, and significance (*) was determined by two-tailed *t* test ($P < 0.02$).

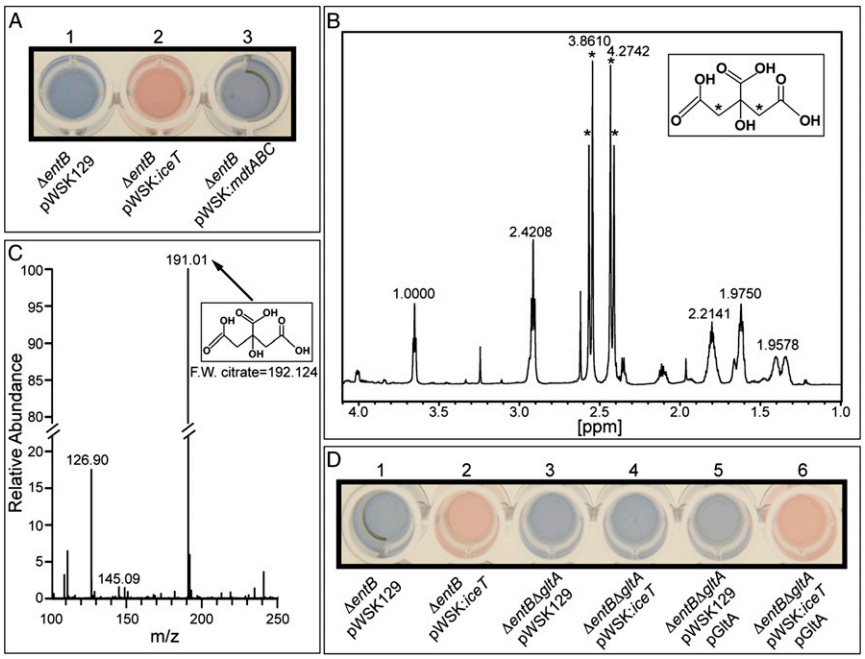

Fig. 5. Cells expressing MdtD(IceT) secrete the CAS-reactive iron chelator citrate. (*A*) EF341 (Δ*entB*) is unable to produce siderophores and is CAS-negative (well 1). Expression of MdtD(IceT) (EF342) results in secretion of a CAS-positive iron chelator (well 2), whereas expression of MdtABC (EF336) does not (well 3). (*B*) The CAS-positive fraction was purified from growth medium and analyzed by ^{1}H NMR. Peaks indicated by an asterisk correspond to hydrogen atoms bound to the 1 and 3 carbons of citrate (indicated by an asterisk in *Inset*). (*C*) Identification of citrate was confirmed by determining the mass of the compound by mass spectrometry. MdtD was therefore renamed IceT. (*D*) Supernatant from EF345 and EF346 lacking citrate synthase (Δ*entB* Δ*gltA*, wells 3 and 4) are not CAS-positive even though EF346 expresses IceT (compare wells 2 and 4). When citrate synthase is expressed from a plasmid (EF347 and EF348, wells 5 and 6), IceT-dependent secretion of the chelator is restored (well 6).

The final active fraction generated from EF342 supernatant was analyzed by ^{1}H NMR spectroscopy (Fig. 5*B*) and mass spectrometry (Fig. 5*C*). The CAS-reactive molecule was identified as citrate, a known iron chelator. To genetically confirm this identification, a citrate synthase mutation (Δ*gltA*) was constructed. When MdtD(IceT) was expressed in a Δ*entB* Δ*gltA* background (EF346), the medium was no longer CAS-positive (Fig. 5*D*, lane 4). Expression of GltA from a plasmid to restore citrate synthase function restored secretion of the chelator in an MdtD(IceT)-dependent manner (Fig. 5*D*, lanes 5 and 6). Identification of citrate as the iron chelator led us to redesignate MdtD as IceT.

Expression of IceT Protects *S.* Typhimurium Against Clinically Relevant Antibiotics. Citrate is the product of the initial step in the tricarboxylic acid (TCA) cycle. Thus, we hypothesized that IceT-mediated efflux of citrate might slow metabolism and growth. Indeed, when EF35 was grown in M9 to promote flux through the TCA cycle, and IceT expression was induced, growth decreased dramatically before arresting completely 1.5–2.0 h postinduction (Fig. S5*A*). The growth rate of EF35 in LB was also reduced upon IceT expression, although growth was not completely arrested due to the availability of alternative carbon sources. When the citrate content of the growth medium was quantified 60 and 120 min after IceT induction, net efflux rates of 2.70×10^5 molecules per cell^{-1} min^{-1} and 1.04×10^5 molecules per cell^{-1} min^{-1} were calculated for those time intervals (Fig. S5*B*). In comparison, *Escherichia coli* cells growing exponentially on glucose have been found to contain 2 mM citrate or $\sim 7.8 \times 10^5$ molecules per cell (40). Studies in *Mycobacterium tuberculosis* have shown that redirection of acetyl-CoA from the TCA cycle to triglyceride synthesis not only reduces carbon flux through the TCA cycle, slowing growth rate, but also increases antibiotic tolerance (41). We reasoned that efflux of citrate via IceT might have a similar effect by reducing both TCA cycle flux and intracellular free iron. EF355 and EF356 were treated with the β-lactam ampicillin (Fig. 6*A*), and EF39 and EF35 were treated with the fluoroquinolone ciprofloxacin (Fig. 6*B*), antibiotics routinely used to treat *Salmonella* infections. Survival was determined by plating and enumeration of cfu at various time points posttreatment. Survival of IceT-expressing strains was significantly greater following antibiotic treatment than that of strains carrying empty vector. Thus, IceT expression can increase tolerance to clinically relevant antibiotics of diverse functional classes.

Discussion

Here we report that induced expression of a previously uncharacterized transporter designated IceT results in citrate efflux, reduced intracellular iron content, and reduced susceptibility to oxidative stress, nitrosative stress, and antimicrobial agents of diverse classes. IceT appears to constitute an efflux system that links central metabolism with stress resistance.

Availability of citrate has significant metabolic implications for the cell. Stress-induced redirection of acetyl-CoA away from citrate synthase to triacylglycerol synthesis in *M. tuberculosis* leads to reduced flux through the TCA cycle and increased antibiotic tolerance (41). Efflux of citrate by IceT in Gram-negative bacteria may represent an analogous mechanism of metabolic control. Based on measured efflux of iron and citrate (Fig. 4 *B* and *C* and Figs. S3*B* and S5*B*), IceT appears to be capable of exporting either iron citrate or citrate alone, and citrate efflux is sufficient to curtail growth. Lower levels of IceT expression and

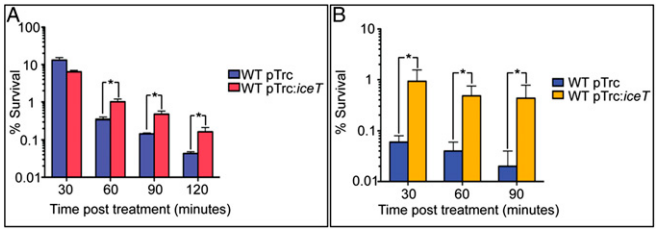

Fig. 6. IceT expression protects *S.* Typhimurium against the antibiotics ampicillin and ciprofloxacin. (*A*) EF356 expressing IceT (red) is less susceptible to ampicillin than EF355 containing empty vector (blue) at 30 min $P = 0.0065$, 60 min $P = 0.0039$, 90 min $P = 0.0046$, and 120 min $P = 0.014$. (*B*) EF35 expressing IceT (gold) is less susceptible to ciprofloxacin than EF39 containing empty vector (blue) at 30 min $P = 0.0086$, 60 min $P = 0.0028$, and 90 min $P = 0.0055$. Data are the mean of three replicates ±1 SD and significance (*) was determined by two-tailed *t* test.

supplementation with alternative carbon sources (i.e., amino acids) are permissive for growth.

Expression of IceT leads to reduced levels of total intracellular iron. Two possible explanations for this observation are that citrate efflux interferes with iron uptake by FeoAB or that citrate efflux by IceT facilitates efflux of free intracellular iron. The amount of citrate effluxed by IceT-expressing cells increased the citrate concentration in the medium to only 60–80 μM, whereas iron was present at concentrations of 1–2 mM. It therefore appears unlikely that citrate could significantly inhibit uptake by chelation. Though it remains formally possible that uptake is inhibited by an alternative mechanism, we observed that IceT expression leads to reduced intracellular iron even in the absence of FeoAB overexpression (Fig. S3*B*). Citrate is capable of binding both Fe(II) and Fe(III) in mononuclear complexes (42). Citrate binds Fe(II) with much lower affinity, however (43), and it is presently unclear how cytosolic Fe(II) can be exported by the IceT transporter. Perhaps chelation by citrate promotes the oxidation of Fe(II) to Fe(III), as has been demonstrated for desferrioxamine (23).

A system for removal of free intracellular iron may have evolved in response to stresses encountered by pathogenic bacteria during infection. IceT is highly conserved throughout the Enterobacteriaceae with characteristic iron-liganding residues, including a cysteine, a tyrosine, and a pair of histidines (Fig. S6). Though iron sequestration is an important host defense mechanism, and iron availability can affect virulence, host immune cells also release ROS and RNS that can penetrate bacterial cells and mobilize iron from iron–sulfur (Fe–S) centers and other iron-containing proteins. Through Fenton chemistry, free iron can catalyze the formation of oxyradicals that damage DNA and proteins. Reduction of intracellular free iron levels confers resistance to diverse stress conditions that act through a final common pathway of oxyradical formation. Although iron citrate export has yet to be directly demonstrated, the ability of IceT to ameliorate iron-dependent toxicity and reduce levels of total cellular iron, along with the known properties of citrate as an iron chelator, are consistent with such a mechanism.

In *S*. Typhimurium and many other enteric bacteria, expression of IceT is coregulated with the RND superfamily transporter MdtABC, which mediates multidrug efflux (35). Because antimicrobial agents may be potentiated by ROS (2), the coordinate expression of drug and iron citrate efflux systems could both remove toxic agents and ameliorate their cytotoxic actions. MdtABC and IceT expression are regulated by the BaeSR two-component regulatory system, which has been implicated in extracytoplasmic stress resistance in *E. coli* (30, 44). Although the mechanism of BaeSR activation remains to be elucidated, the present study shows that nitrosative stress and dysregulation of iron metabolism lead to expression of the *mdtABC iceT baeSR* operon, consistent with a role in defense against free iron-mediated cytotoxicity and host-associated stresses, whereas work by others has shown induction of expression by the antibiotic ciprofloxacin (45).

The present study demonstrates that in addition to protecting *S*. Typhimurium from oxidative and nitrosative stresses and iron-mediated cytotoxicity, IceT overexpression also renders *Salmonella* less susceptible to killing by the clinically important antibiotics ampicillin and ciprofloxacin. Studies have shown that both restriction of iron availability and early blocks in the TCA cycle lead to increased antibiotic tolerance (2, 46). Our observations are in agreement with these previous studies and demonstrate a unique mechanism in which regulation of metabolic flux, cellular redox state, and intracellular iron levels can be modulated by a single protein to confer stress resistance and antibiotic tolerance.

Materials and Methods

Growth Conditions. Bacteria were grown aerobically in LB (Difco) or M9 medium (1× Difco M9 salts, 0.1 mM $CaCl_2$, 2 mM $MgSO_4$, 0.4% glucose) at 37 °C with shaking at 250 rpm. Antibiotic concentrations were as follows unless stated otherwise: 100 μg mL^{-1} ampicillin, 50 μg mL^{-1} kanamycin (kan), and 20 μg mL^{-1} chloramphenicol. Gene expression from P_{trc} was induced with 1 mM IPTG. Gene expression from P_{araBAD} was induced with 0.2% arabinose.

Strain and Plasmid Construction. Plasmids, strains, and primers are listed in Tables S1 and S2. For detailed construction, see *SI Materials and Methods*. Deletions were generated using the lambda Red method (47), and all mutations were transduced into a clean *S*. Typhimurium ATCC 14028s background using P22 bacteriophage. *E. coli* strain DH10B was the host strain for all cloning; confirmed plasmids were electroporated into *S*. Typhimurium.

Transposon Mutant Library Screening. An *S*. Typhimurium MudJ transposon mutant library was replica-plated onto LB and LB SN (0.5 μg mL^{-1}). Hypersusceptible mutants, identified by growth inhibition on LB SN, were confirmed by repatching. Ten candidates were identified from ∼10,000 mutants screened. Insertion locations were determined by amplifying and sequencing adjacent genomic DNA as described previously (48).

Streptonigrin Susceptibility. EF3 and EF221 were grown overnight in 5 mL LB, diluted 1:10 in fresh LB, then diluted 1:10 into LB SN for a final concentration of 6 μg mL^{-1} and volume of 300 μL in a microtiter plate. Cells were grown in a Labsystems Bioscreen C machine (Growth Curves USA) that measured OD_{600} every 15 min.

Nitric Oxide Susceptibility and Induction. NONOates were solubilized in 0.01 M sodium hydroxide. EF3 and EF221 were grown overnight in 5 mL LB, diluted 1:10 in M9, then diluted 1:10 in M9, 1 mM DEA/NO, and 2 mM Sper/NO for a final volume of 200 μL in a microtiter plate. Cells were grown in a Labsystems Bioscreen C machine with OD_{600} measured every 15 min. To measure NO··induced gene expression, EF3 was grown overnight in 5 mL M9, diluted 1:100 in 100 mL M9, and then grown to OD_{600} 1.5. The 10-mL aliquots were treated with a 1 mM DEA mock treatment, 1 mM DEA/NO, or left untreated. After 20 min, 500 μL of culture were added to 1 mL RNA Protect (Qiagen), and then RNA was isolated using the Qiagen RNeasy Mini Kit and cDNA synthesized using the Qiagen QuantiTect reverse transcription kit. The QuantiFast SYBR Green Kit (Qiagen) was used for quantitative PCR (qPCR). Primers for *mdtA*, *mdtB*, and *mdtD* were described previously (35), and *rpoD* was used as an internal control.

Δ*fur* Induction. EF3 and EF394 were grown overnight in 5 mL LB, diluted 1:1,000 in 25 mL LB, and grown to OD_{600} 1.0. RNA and cDNA were prepared and qPCR performed as described above. For primers, see Table S2.

Bacterial Killing Assays. Strains were grown overnight in 5 mL LB with the appropriate antibiotic, then diluted 1:100 in 25 mL LB with antibiotic. For iron and ciprofloxacin experiments, cells were grown to OD_{600} 0.5 before induction of protein expression for 1 h. For hydrogen peroxide, streptonigrin, and ampicillin experiments, cells were grown for 1 h (OD_{600} 0.2–0.3) and then induced for 1 h (final OD_{600} 0.5–0.6). Following induction, 1-mL aliquots were divided into 18 × 150-mm culture tubes containing the appropriate treatment, then returned to shaking at 37 °C for the duration of the experiment. Percent survival was determined by serially diluting 20 μL culture 1:10 in sterile PBS and plating in triplicate for enumeration of cfu on LB agar. Percent survival was calculated compared with untreated cells.

ICP-MS. For the experiment in Fig. 4*B*, strains HR111 and HR112 were grown as for the iron-killing assay. After induction, 1 mM $FeSO_4$ in ascorbate was added to the medium for 30 min. For the experiment in Fig. 4*C*, subcultured HR111 and HR112 were grown to OD_{600} 0.5–0.6, *feoAB* expression was induced for 1 h, 1 mM $FeSO_4$ was added for 30 min, and then IceT expression was induced for 90 min. Cells were pelleted by centrifugation, washed twice with 25 mL 1-mM EDTA and once with 1 mL 1-mM EDTA, followed by a high-speed spin to remove all supernatant. Pellets were resuspended in 1 mL analytical grade nitric acid and incubated at 85 °C for 45 min. Remaining cell debris was removed by centrifugation at 21,000 × *g* for 15 min, and the nitric acid solution was diluted 1:10 in MilliQ purified water. ICP-MS analysis was conducted by the Environmental Health Laboratory and Trace Organics Analysis Center at the University of Washington.

CAS Assay. Strains were grown 8 h in 5 mL LB kan, pelleted by centrifugation, washed twice with M9, and then subcultured 1:100 in M9 kan 0.4% casamino acids and grown 12–16 h. All cultures reached a similar OD_{600}. Cells were pelleted by centrifugation and the cell-free supernatant used for CAS assays (39). For CAS shuttle solution, 9 mL of 0.167 mM $FeCl_3$, 1.67 mM HCl, and 1.67 mM CAS were slowly added to 40 mL of 1.3 mM hexadecyltrimethylammonium bromide. The combined solution was then added to 36.5 mL of 1.37 M piperazine at pH 5.6, and the final volume adjusted to 100 mL with water. To activate the CAS shuttle solution, 400 μL of 1 M 5-sulfosalicylic acid was added and the solution stored in the dark until use. One hundred microliters of CAS shuttle solution was combined with 100 μL of cell-free supernatant in a 96-well microtiter plate and allowed to react for 5–10 min.

Biochemical Characterization of the Chelator. Cell-free supernatants from EF341 and EF342 were prepared as described above, then evaporated under reduced pressure with 2% wt/vol HP-20 resin (Diaion). The resin was applied to a 300-mL HP-20 column and elution fractions in 2 L water, 2 L 10% vol/vol methanol, and 2 L 100% methanol were collected. The CAS-active water fraction was loaded onto a C18 column (10 × 100 mm; Atlantis T3 prep) and eluted with a gradient of 0–50% vol/vol methanol, 0.1% trifluoroacetic acid with a flow rate of 4 mL min^{-1}. Fractions were collected every 30 s from 0.5 to 15 min. Active fractions were combined, loaded on a 100-mL Sephadex LH-20 column, and eluted with 30% vol/vol methanol. Active subfractions were combined and separated by semipreparative HPLC over a 10 × 100-mm Atlantis T3 prep column by eluting with water to yield an active peak. Peak components were identified by ^1H NMR and mass spectrometry. A small amount of lysine was present in the fraction but found to be inactive as a chelator.

ACKNOWLEDGMENTS. We thank Susan McKusker at McMaster University for technical assistance with the chelator identification; Joyce Karlinsey at the University of Washington for technical assistance with strain construction and mutant complementation; Kelly McCusker at the University of Washington for advice on rate calculation; Jim Imlay at the University of Illinois for constructive conversations regarding the chemistry of iron and citrate; and Shelley Payne at the University of Texas for helpful suggestions. Support for this work was provided by National Institutes of Health Grants AI39557, AI44486, and AI77629 (to F.C.F.), and National Institutes of Health Fellowship AI54052 (to M.L.C.).

1. Dwyer DJ, Kohanski MA, Hayete B, Collins JJ (2007) Gyrase inhibitors induce an oxidative damage cellular death pathway in *Escherichia coli*. *Mol Syst Biol* 3:91.
2. Kohanski MA, Dwyer DJ, Hayete B, Lawrence CA, Collins JJ (2007) A common mechanism of cellular death induced by bactericidal antibiotics. *Cell* 130(5):797–810.
3. Kohanski MA, Dwyer DJ, Wierzbowski J, Cottarel G, Collins JJ (2008) Mistranslation of membrane proteins and two-component system activation trigger antibiotic-mediated cell death. *Cell* 135(4):679–690.
4. Kohanski MA, Dwyer DJ, Collins JJ (2010) How antibiotics kill bacteria: From targets to networks. *Nat Rev Microbiol* 8(6):423–435.
5. Foti JJ, Devadoss B, Winkler JA, Collins JJ, Walker GC (2012) Oxidation of the guanine nucleotide pool underlies cell death by bactericidal antibiotics. *Science* 336(6079):315–319.
6. Keren I, Wu Y, Inocencio J, Mulcahy LR, Lewis K (2013) Killing by bactericidal antibiotics does not depend on reactive oxygen species. *Science* 339(6124):1213–1216.
7. Liu Y, Imlay JA (2013) Cell death from antibiotics without the involvement of reactive oxygen species. *Science* 339(6124):1210–1213.
8. Marquet A, Bui BT, Smith AG, Warren MJ (2007) Iron-sulfur proteins as initiators of radical chemistry. *Nat Prod Rep* 24(5):1027–1040.
9. Beinert H, Holm RH, Münck E (1997) Iron-sulfur clusters: Nature's modular, multipurpose structures. *Science* 277(5326):653–659.
10. Puschmann M, Ganzoni AM (1977) Increased resistance of iron-deficient mice to *Salmonella* infection. *Infect Immun* 17(3):663–664.
11. Kochan I, Wasynczuk J, McCabe MA (1978) Effects of injected iron and siderophores on infections in normal and immune mice. *Infect Immun* 22(2):560–567.
12. Sawatzki G, Hoffmann FA, Kubanek B (1983) Acute iron overload in mice: Pathogenesis of *Salmonella typhimurium* infection. *Infect Immun* 39(2):659–665.
13. Collins HL, Kaufmann SH, Schaible UE (2002) Iron chelation via deferoxamine exacerbates experimental salmonellosis via inhibition of the nicotinamide adenine dinucleotide phosphate oxidase-dependent respiratory burst. *J Immunol* 168(7):3458–3463.
14. Finkelstein RA, Sciortino CV, McIntosh MA (1983) Role of iron in microbe-host interactions. *Rev Infect Dis* 5(Suppl 4):S759–S777.
15. Schaible UE, Kaufmann SH (2004) Iron and microbial infection. *Nat Rev Microbiol* 2(12):946–953.
16. Luckey M, Pollack JR, Wayne R, Ames BN, Neilands JB (1972) Iron uptake in *Salmonella typhimurium*: Utilization of exogenous siderochromes as iron carriers. *J Bacteriol* 111(3):731–738.
17. Pollack JR, Ames BN, Neilands JB (1970) Iron transport in *Salmonella typhimurium*: Mutants blocked in the biosynthesis of enterobactin. *J Bacteriol* 104(2):635–639.
18. Crouch ML, Castor M, Karlinsey JE, Kalhorn T, Fang FC (2008) Biosynthesis and IroC-dependent export of the siderophore salmochelin are essential for virulence of *Salmonella enterica* serovar Typhimurium. *Mol Microbiol* 67(5):971–983.
19. Halliwell B, Gutteridge JM (1992) Biologically relevant metal ion-dependent hydroxyl radical generation. An update. *FEBS Lett* 307(1):108–112.
20. Imlay JA (2002) How oxygen damages microbes: Oxygen tolerance and obligate anaerobiosis. *Adv Microb Physiol* 46:111–153.
21. Imlay JA (2003) Pathways of oxidative damage. *Annu Rev Microbiol* 57:395–418.
22. Imlay JA (2006) Iron-sulphur clusters and the problem with oxygen. *Mol Microbiol* 59(4):1073–1082.
23. Keyer K, Imlay JA (1996) Superoxide accelerates DNA damage by elevating free-iron levels. *Proc Natl Acad Sci USA* 93(24):13635–13640.
24. Fang FC (2004) Antimicrobial reactive oxygen and nitrogen species: concepts and controversies. *Nat Rev Microbiol* 2(10):820–832.
25. Ren B, Zhang N, Yang J, Ding H (2008) Nitric oxide-induced bacteriostasis and modification of iron-sulphur proteins in *Escherichia coli*. *Mol Microbiol* 70(4):953–964.
26. Duan X, Yang J, Ren B, Tan G, Ding H (2009) Reactivity of nitric oxide with the [4Fe-4S] cluster of dihydroxyacid dehydratase from *Escherichia coli*. *Biochem J* 417(3):783–789.
27. Fang FC (2011) Antimicrobial actions of reactive oxygen species. *MBio* 2(5):e00141-11.
28. Yeowell HN, White JR (1982) Iron requirement in the bactericidal mechanism of streptonigrin. *Antimicrob Agents Chemother* 22(6):961–968.
29. Baranova N, Nikaido H (2002) The *baeSR* two-component regulatory system activates transcription of the *yegMNOB* (*mdtABCD*) transporter gene cluster in *Escherichia coli* and increases its resistance to novobiocin and deoxycholate. *J Bacteriol* 184(15):4168–4176.
30. Leblanc SK, Oates CW, Raivio TL (2011) Characterization of the induction and cellular role of the BaeSR two-component envelope stress response of *Escherichia coli*. *J Bacteriol* 193(13):3367–3375.
31. Nagakubo S, Nishino K, Hirata T, Yamaguchi A (2002) The putative response regulator BaeR stimulates multidrug resistance of *Escherichia coli* via a novel multidrug exporter system, MdtABC. *J Bacteriol* 184(15):4161–4167.
32. Hirakawa H, Nishino K, Yamada J, Hirata T, Yamaguchi A (2003) Beta-lactam resistance modulated by the overexpression of response regulators of two-component signal transduction systems in *Escherichia coli*. *J Antimicrob Chemother* 52(4):576–582.
33. Appia-Ayme C, et al. (2011) Novel inducers of the envelope stress response BaeSR in *Salmonella* Typhimurium: BaeR is critically required for tungstate waste disposal. *PLoS ONE* 6(8):e23713.
34. Hirakawa H, Inazumi Y, Masaki T, Hirata T, Yamaguchi A (2005) Indole induces the expression of multidrug exporter genes in *Escherichia coli*. *Mol Microbiol* 55(4):1113–1126.
35. Nishino K, Nikaido E, Yamaguchi A (2007) Regulation of multidrug efflux systems involved in multidrug and metal resistance of *Salmonella enterica* serovar Typhimurium. *J Bacteriol* 189(24):9066–9075.
36. Bjarnason J, Southward CM, Surette MG (2003) Genomic profiling of iron-responsive genes in *Salmonella enterica* serovar Typhimurium by high-throughput screening of a random promoter library. *J Bacteriol* 185(16):4973–4982.
37. McHugh JP, et al. (2003) Global iron-dependent gene regulation in *Escherichia coli*. A new mechanism for iron homeostasis. *J Biol Chem* 278(32):29478–29486.
38. Velayudhan J, Castor M, Richardson A, Main-Hester KL, Fang FC (2007) The role of ferritins in the physiology of *Salmonella enterica* sv. Typhimurium: A unique role for ferritin B in iron-sulphur cluster repair and virulence. *Mol Microbiol* 63(5):1495–1507.
39. Schwyn B, Neilands JB (1987) Universal chemical assay for the detection and determination of siderophores. *Anal Biochem* 160(1):47–56.
40. Bennett BD, et al. (2009) Absolute metabolite concentrations and implied enzyme active site occupancy in *Escherichia coli*. *Nat Chem Biol* 5(8):593–599.
41. Baek SH, Li AH, Sassetti CM (2011) Metabolic regulation of mycobacterial growth and antibiotic sensitivity. *PLoS Biol* 9(5):e1001065.
42. Francis AJ, Dodge CJ (1993) Influence of complex structure on the biodegradation of iron-citrate complexes. *Appl Environ Microbiol* 59(1):109–113.
43. Field TB, McCourt JL, McBryde WAE (1974) Composition and stability of iron and copper citrate complexes in aqueous solution. *Can J Chem* 52(17):3119–3124.
44. Raffa RG, Raivio TL (2002) A third envelope stress signal transduction pathway in *Escherichia coli*. *Mol Microbiol* 45(6):1599–1611.
45. Guerrero P, et al. (2012) Characterization of the BaeSR two-component system from *Salmonella* Typhimurium and its role in ciprofloxacin-induced *mdtA* expression. *Arch Microbiol* 194(6):453–460.
46. Dwyer DJ, Kohanski MA, Collins JJ (2009) Role of reactive oxygen species in antibiotic action and resistance. *Curr Opin Microbiol* 12(5):482–489.
47. Datsenko KA, Wanner BL (2000) One-step inactivation of chromosomal genes in *Escherichia coli* K-12 using PCR products. *Proc Natl Acad Sci USA* 97(12):6640–6645.
48. Pomposiello PJ, Demple B (2000) Identification of SoxS-regulated genes in *Salmonella enterica* serovar Typhimurium. *J Bacteriol* 182(1):23–29.